

Orientation-Controlled Single-Molecule Junctions**

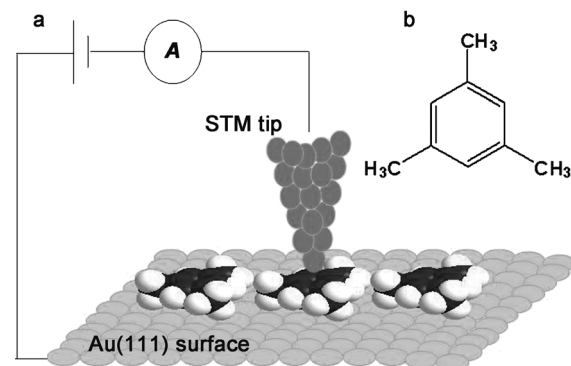
Sepideh Afsari, Zhihai Li, and Eric Borguet*

Abstract: The conductivity of a single aromatic ring, perpendicular to its plane, is determined using a new strategy under ambient conditions and at room temperature by a combination of molecular assembly, scanning tunneling microscopy (STM) imaging, and STM break junction (STM-BJ) techniques. The construction of such molecular junctions exploits the formation of highly ordered structures of flat-oriented mesitylene molecules on Au(111) to enable direct tip/π contacts, a result that is not possible by conventional methods. The measured conductance of Au/π/Au junction is about $0.1 G_0$, two orders of magnitude higher than the conductance of phenyl rings connected to the electrodes by standard anchoring groups. Our experiments suggest that long-range ordered structures, which hold the aromatic ring in place and parallel to the surface, are essential to increase probability of the formation of orientation-controlled molecular junctions.

Molecular-scale electronic devices usually are designed by wiring a single molecule between two metal electrodes^[1,2] most commonly using mechanically controlled break junctions (MCBJ), or scanning probe microscopy, for example, scanning tunneling microscopy (STM). Single-molecule conductance (SMC) studies are carried out in ultrahigh vacuum (UHV)^[3–7] or under ambient conditions^[8–13] and focus on molecules with functional groups that provide efficient electronic coupling and bind the organic molecular backbone to the electrodes.^[14] However, conductance is sensitive to the atomic level details of the molecule–electrode contact^[15] so that the anchoring groups typically end up decreasing the single-molecule junction conductivity. Thus, creating well-defined, highly conductive molecular junctions is challenging.^[16–23]

Another strategy, demonstrated in this study, is to use the stabilization provided by long-range ordered structures that fix the molecular geometry on the electrode. The templates formed by the ordered molecular adlayer facilitate SMC measurements of single-molecule junctions with controlled molecular orientation that cannot be formed by conventional methods.

Mesitylene (1,3,5-trimethylbenzene, Scheme 1b) is a typical solvent for SMC measurements because of its perceived



Scheme 1. a) Single mesitylene junction formed by direct interaction of the Au electrodes to the aromatic ring; b) Molecular structure of mesitylene.

inability to form molecular junctions.^[24–27] Methyl groups are not effective anchoring groups.^[28] Hence, the conductance of single mesitylene molecules has not been reported so far. Here, we apply a novel strategy to create highly conductive Au/mesitylene/Au junctions by means of direct contact between the π system of mesitylene and the gold electrodes. We show that mesitylene can form long-range ordered structures with the aromatic ring lying flat on Au(111), facilitating the creation of junctions that measure the conductance perpendicular to the plane of the benzene ring (Scheme 1a) under ambient conditions. The single molecule conductance of this Au/π/Au junction is about $0.1 G_0$, 100-fold more conductive than junctions formed by benzene rings connected by typical standard linkers, for example, thiols or amines.^[14,29,30]

Our high-resolution STM images show that mesitylene forms a long-range ordered structure on Au(111) (Figure 1a). A closer look at the STM images (Figure 1b), as well as the corresponding cross sections (see Figure S1 in the Supporting

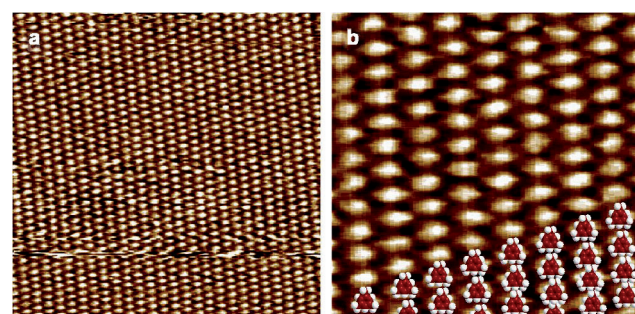


Figure 1. STM images of mesitylene on Au(111); a) $20 \times 20 \text{ nm}^2$ and b) $6 \times 6 \text{ nm}^2$ with superimposed mesitylene structure; $V_{\text{bias}} = -0.10 \text{ V}$, $I_t = 10 \text{ nA}$.

[*] S. Afsari, Dr. Z. Li, Prof. Dr. E. Borguet
Department of Chemistry, Temple University
Philadelphia, PA 19122 (USA)
E-mail: eborguet@temple.edu
Homepage: <http://www.temple.edu/borguet/>

[**] We thank Dr. Yangjun Xing for help with the software used for statistical analysis and fitting of the SMC data. Financial support from NSF (grant CHE0809838) is gratefully acknowledged.

Supporting information for this article is available on the WWW under <http://dx.doi.org/10.1002/anie.201402343>.

Information), reveals that mesitylene lies flat on the gold surface. Considering the facts that methyl groups have weak intermolecular interactions, and that mesitylene self-assembles into a closed packed structure on the Au(111), we concluded that the dominant force for long-range-ordered structure formation is the substrate/molecule interaction between the gold surface and π -structure of mesitylene, not intermolecular interactions.

In STM-BJ experiments, every time the STM tip is brought into contact with the Au surface, it contacts the ordered adlayer of mesitylene in order to form junctions (Scheme 1). According to the STM images, while the STM tip is pulling out of the surface, the most probable geometry of single-molecule junctions is with the mesitylene molecule sandwiched between the two Au electrodes by direct contact to the π system. We hypothesize that because of the stabilizing effect of the ordered monolayer, the mesitylene molecules are held in place on the Au(111) as the junction forms. This results in single-molecule junctions with a reproducible geometry where the phenyl ring is perpendicular to the STM tip.

STM-BJ experiments of mesitylene with Au electrodes (in the range of 0–10000 nA and at a bias of –0.10 V), revealed two peaks in the corresponding histogram (Figure 2): 1) The peak of quantum conductance ($G_0 = 2e^2h = 7.75 \times 10^{-5}$ S),^[31] because of repeated forming and breaking of gold point contacts; 2) another peak with a conductance one order of magnitude lower ($\approx 0.1 G_0$), which is associated with the conductivity of single mesitylene molecules in junctions. Repeated experiments in mesitylene reproduced the $\approx 0.1 G_0$ peak with an average value of $0.125 G_0 (\pm 0.006)$ as well as the G_0 peak (Table S1 and Figure S2).

One may note that: 1) The conductivity of the benzene derivatives reported so far with Au electrodes are mostly in the range of 0.001 – $0.01 G_0$,^[14,29–30] and 2) the methyl group is known as a poor anchoring group for gold electrodes.^[28] Thus,

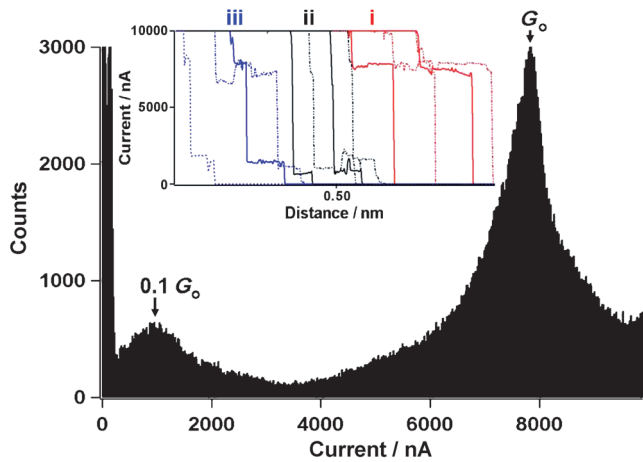


Figure 2. All-data point current histogram of STM-BJ in mesitylene determined from experiments carried out at $V_{\text{bias}} = -0.10$ V without any data selection of 9086 individual current–distance curves. Inset: Individual current–distance curves: conductance in range of G_0 (type (i), red), about $0.1 G_0$ (type (ii), black), and conductance of $0.1 G_0$ and G_0 (type (iii), blue).

the conductivity in the range of $0.1 G_0$ cannot be attributed to a mesitylene molecule bridging between gold electrodes via gold-methyl contacts (unless these have remarkably LOW contact resistance). Instead, we tentatively assign this high conductance signature to the conductance of Au/mesitylene/Au junction, with the STM tip perpendicular to the mesitylene phenyl ring. This hypothesis is supported by calculations, which estimate that the conductance in the π -stack direction for a single benzene ring placed between two Au electrodes is about $10 \mu\text{S}$ ($0.13 G_0$).^[32] This value is very close to the average value of $0.125 G_0 (\pm 0.006)$ observed in our data. Since methyl groups have a lesser perturbing effect on the electronic structure of the aromatic ring, compared to other functional groups except H, we expect that the measured conductivity perpendicular to the molecular plane of the aromatic ring of mesitylene should be very close to that of benzene. Thus, we assigned the $0.1 G_0$ peak (Figure 2) to the conductivity of Au/mesitylene/Au junctions with the aromatic ring perpendicular to the junction axis (Scheme 1a).

The STM-BJ technique has been employed previously to measure the single-molecule conductance of multiple π - π stacked aromatic rings, revealing an exponential decay of the conductance with an increasing number of stacked benzene rings.^[33] It has been reported that the junction is formed because of contacts between the gold electrodes and the outer benzene rings of 2,3, and 4 π -stacked molecules,^[33] resulting in a measured conductivity in the range of $10^{-2} G_0$, $10^{-3} G_0$ and $10^{-4} G_0$, respectively.^[33] This leads us to hypothesize, assuming a linear trend for conductivity versus the number of π -stacks, a conductivity in the range of $10^{-1} G_0$ for an Au/aromatic ring/Au junction. Thus, both theory and experiments are consistent with the $0.125 G_0 (\pm 0.006)$ conductance observed for a single aromatic ring perpendicular to the molecular plane for mesitylene molecule.

STM images of the mesitylene monolayer on Au(111) taken after running STM-BJ experiments, show two kinds of defects in the monolayer: defects with a size of several molecules and defects with the size of only one molecule (Figure 3 a and b). These defects most likely formed when the gold tip contacted the molecular monolayer. If the very sharp STM tip gently touches the monolayer but does not form a single gold atom contact, defects one or two mesitylene molecules in size can form in the monolayer. When the STM tip is pulled off the surface a single mesitylene traps in the junction. The most probable geometry for the mesitylene in

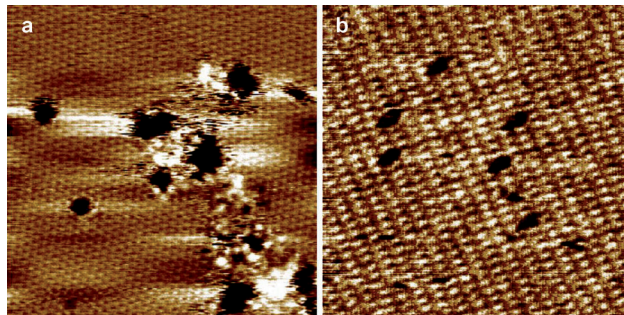


Figure 3. STM images of mesitylene on Au(111) after running STM-BJ experiment, $V_{\text{bias}} = -0.10$ V, $I_t = 10$ nA. a) $30 \times 30 \text{ nm}^2$, b) $20 \times 20 \text{ nm}^2$.

the junction is with the aromatic ring perpendicular to the STM tip.

A closer look at the individual current-distance curves (Figure 2, inset) showed that there are three types of curves: i) curves with only high conductance current steps with conductivity in the range of G_0 ; ii) curves with only low conductance current type with conductivity in the range of $0.1 G_0$ and iii) curves with both types of features, that is, $0.1 G_0$ and G_0 . We suggest that type (i) current steps are due to a single gold atom bridging between two gold electrodes (G_0) when the STM tip lands on the bare gold surface in defective parts of the monolayer (Figure 3a). In addition, mesitylene molecules may bridge the gold electrodes with a perpendicular geometry before the gold contact is broken. This phenomenon could be responsible for current-distance curves of type (iii) where both molecular and atomic junctions simultaneously exist.

Current histogram analysis (Figure S2) reveals the presence of a high current shoulder on the quantum conductance peak (G_0). This suggests that the formation of a self-assembled monolayer on the Au electrode increases the conductivity of the surface beyond the single gold atom conductance (G_0) due to the simultaneous formation of single mesitylene and single gold atom junctions resulting combined atomic and molecular conductance in parallel ($0.1 G_0 + G_0$).

In order to confirm the reproducibility of the mesitylene conductance peak, and to verify that it actually represented the signature of molecular conductance, we investigated the current-bias relationship for this mesitylene conductance feature. As the bias voltage (V_{bias}) was varied, the current maximum in histograms increases, showing a quasi-linear V_{bias} dependence, that is, the molecular junction conductance remains relatively constant in this bias range (Figure 4).

For investigating the hypothesis that the long-range ordered structure of mesitylene facilitates the formation of junctions with the aromatic ring perpendicular to the STM tip, we conducted a series of STM-BJ experiments using other

benzene derivative solvents (benzene, toluene, and 1,2,4-trichlorobenzene) for comparison, as well as a mesitylene solution initially heated up to 90°C as a control (detailed analysis in the Supporting Information) where long-range ordered structure of mesitylene was not observed (Figure S4d). Toluene and 1,2,4-trichlorobenzene are typical organic solvents for SMC measurements.^[28,34–36]

The conductance histogram of benzene shows a clear G_0 peak but no other dominant molecular conductance peak (Figure S3a), which can be rationalized as a consequence of benzene not having any anchoring groups to connect to gold electrode and the inability of benzene to form ordered 2D structures at room temperature. Molecular conductance peaks were not observed for benzene in previous studies when using gold electrodes either, even under UHV and low temperature.^[17]

In the case of toluene, 1,2,4-trichlorobenzene, and mesitylene initially heated up to 90°C, histograms did not reveal a well-defined current peak that could be associated with a molecular feature (Figures S3c, S3d, and S5). The hypothesis that long range ordered structure causes the molecule to orient with its plane perpendicular to the junction is well supported by comparison of STM images of the Au(111) in 1,2,4-trichlorobenzene, toluene and mesitylene (Figure S4). Only when mesitylene formed long range ordered structures on the Au(111), featuring large domains of an almost defect free closed pack lattice, did a dominant $0.1G_0$ molecular conductance peak appear. Thus, we concluded that the presence of an ordered self-assembled monolayer increases the probability of single mesitylene molecules being sandwiched between two gold electrodes with the junction axis perpendicular to the aromatic ring.

In summary, using a combination of STM imaging and STM-BJ techniques, we showed that the existence of an ordered mesitylene adlayer on Au(111) favors the formation of metal-molecule-metal junctions by direct contact between Au and the π system of mesitylene. STM images show long-range ordered structures of mesitylene adsorbed on Au(111) with its molecular plane perpendicular to the Au tip. The measured single-molecule conductance of Au/ π /Au junctions is $0.125 G_0$ (± 0.006), consistent with calculations and two orders of magnitude higher than the measured conductance of a phenyl ring connected by standard anchoring groups.^[14,29–30] We attribute this conductance peak to charge transport perpendicular to the aromatic ring of the mesitylene molecule.

Received: February 12, 2014

Revised: May 21, 2014

Published online: July 15, 2014

Keywords: benzene derivatives · mesitylene · molecular electronics · self-assembly · single-molecule conductivity

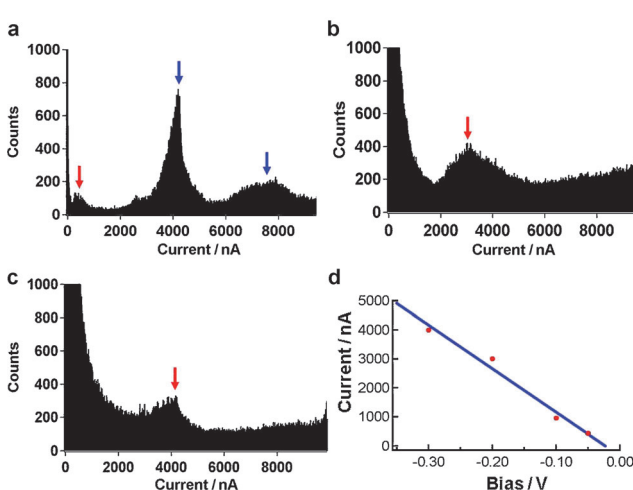


Figure 4. Histogram analysis of STM-BJ in mesitylene, experiments carried out at V_{bias} : a) -0.05 V, b) -0.20 V, c) -0.3 V, d) linear fitting of current versus bias diagram; Peaks for mesitylene and quantum conductance are indicated by red and blue arrows, respectively.

[1] M. Díaz, M. S. Martín-González, J. L. Costa-Krämer, *Surf. Sci.* **2010**, *604*, 1420–1424.

[2] A. H. Flood, J. F. Stoddart, D. W. Steuerman, J. R. Heath, *Science* **2004**, *306*, 2055–2056.

- [3] M. Ruben, A. Landa, E. Lortscher, H. Riel, M. Mayor, H. Gorls, H. B. Weber, A. Arnold, F. Evers, *Small* **2008**, *4*, 2229–2235.
- [4] F. von Wrochem, F. Scholz, A. Yasuda, J. M. Wessels, *J. Phys. Chem. C* **2009**, *113*, 12395–12401.
- [5] M. Kiguchi, K. Murakoshi, *J. Phys. Chem. C* **2008**, *112*, 8140–8143.
- [6] S. U. Kim, B. S. Kim, J. C. Park, H. K. Shin, Y. S. Kwon, *Curr. Appl. Phys.* **2006**, *6*, 608–611.
- [7] M. Fujihira, M. Suzuki, S. Fujii, A. Nishikawa, *Phys. Chem. Chem. Phys.* **2006**, *8*, 3876–3884.
- [8] E. Lörtscher, C. J. Cho, M. Mayor, M. Tschudy, C. Rettner, H. Riel, *Phys. Chem. Chem. Phys.* **2011**, *12*, 1677–1682.
- [9] L. A. Zotti, T. Kirchner, J. C. Cuevas, F. Pauly, T. Huhn, E. Scheer, A. Erbe, *Small* **2010**, *6*, 1529–1535.
- [10] Z. H. Li, M. Smeu, M. A. Ratner, E. Borguet, *J. Phys. Chem. C* **2013**, *117*, 14890–14898.
- [11] C. R. Arroyo, E. Leary, A. Castellanos-Gomez, G. Rubio-Bollinger, M. T. Gonzalez, N. Agrait, *J. Am. Chem. Soc.* **2011**, *133*, 14313–14319.
- [12] A. Mishchenko, L. A. Zotti, D. Vonlanthen, M. Burkle, F. Pauly, J. C. Cuevas, M. Mayor, T. Wandlowski, *J. Am. Chem. Soc.* **2011**, *133*, 184–187.
- [13] L. Cui, B. Liu, D. Vonlanthen, M. Mayor, Y. C. Fu, J. F. Li, T. Wandlowski, *J. Am. Chem. Soc.* **2011**, *133*, 7332–7335.
- [14] M. Kiguchi, S. Kaneko, *Phys. Chem. Chem. Phys.* **2012**, *13*, 1116–1126.
- [15] M. P. Nikiforov, U. Zerweck, P. Milde, C. Loppacher, T. H. Park, H. T. Uyeda, M. J. Therien, L. Eng, D. Bonnell, *Nano Lett.* **2008**, *8*, 110–113.
- [16] T. Yelin, R. Vardimon, N. Kuritz, R. Korytár, A. Bagrets, F. Evers, L. Kronik, O. Tal, *Nano Lett.* **2013**, *13*, 1956–1961.
- [17] S. Kaneko, T. Nakazumi, M. Kiguchi, *J. Phys. Chem. Lett.* **2010**, *1*, 3520–3523.
- [18] M. Kiguchi, O. Tal, S. Wohlthat, F. Pauly, M. Krieger, D. Djukic, J. C. Cuevas, J. M. van Ruitenbeek, *Phys. Rev. Lett.* **2008**, *101*, 046801.
- [19] T. Hines, I. Diez-Perez, H. Nakamura, T. Shimazaki, Y. Asai, N. J. Tao, *J. Am. Chem. Soc.* **2013**, *135*, 3319–3322.
- [20] W. B. Chen, J. R. Widawsky, H. Vazquez, S. T. Schneebeli, M. S. Hybertsen, R. Breslow, L. Venkataraman, *J. Am. Chem. Soc.* **2011**, *133*, 17160–17163.
- [21] A. V. Tivanski, Y. F. He, E. Borguet, H. Y. Liu, G. C. Walker, D. H. Waldeck, *J. Phys. Chem. B* **2005**, *109*, 5398–5402.
- [22] Y. J. Xing, T. H. Park, R. Venkatramani, S. Keinan, D. N. Beratan, M. J. Therien, E. Borguet, *J. Am. Chem. Soc.* **2010**, *132*, 7946–7956.
- [23] L. E. Scullion, E. Leary, S. J. Higgins, R. J. Nichols, *J. Phys. Condens. Matter* **2012**, *24*, 9.
- [24] R. Huber, M. T. Gonzalez, S. Wu, M. Langer, S. Grunder, V. Horhoiu, M. Mayor, M. R. Bryce, C. S. Wang, R. Jitchati, C. Schonenberger, M. Calame, *J. Am. Chem. Soc.* **2008**, *130*, 1080–1084.
- [25] A. Mishchenko, D. Vonlanthen, V. Meded, M. Burkle, C. Li, I. V. Pobelov, A. Bagrets, J. K. Viljas, F. Pauly, F. Evers, M. Mayor, T. Wandlowski, *Nano Lett.* **2010**, *10*, 156–163.
- [26] S. Nakashima, Y. Takahashi, M. Kiguchi, *Beilstein J. Nanotechnol.* **2011**, *2*, 755–759.
- [27] S. Grunder, R. Huber, V. Horhoiu, M. T. Gonzalez, C. Schonenberger, M. Calame, M. Mayor, *J. Org. Chem.* **2007**, *72*, 8337–8344.
- [28] X. L. Li, J. He, J. Hihath, B. Q. Xu, S. M. Lindsay, N. J. Tao, *J. Am. Chem. Soc.* **2006**, *128*, 2135–2141.
- [29] M. Kiguchi, H. Nakamura, Y. Takahashi, T. Takahashi, T. Ohto, *J. Phys. Chem. C* **2010**, *114*, 22254–22261.
- [30] M. Kiguchi, S. Miura, K. Hara, M. Sawamura, K. Murakoshi, *Appl. Phys. Lett.* **2006**, *89*, 213104.
- [31] B. Q. Xu, N. J. Tao, *Science* **2003**, *301*, 1221–1223.
- [32] M. Mine, T. Tsutsui, E. Miyoshi, *Jpn. J. Appl. Phys.* **2008**, *47*, 8033–8038.
- [33] S. T. Schneebeli, M. Kamenetska, Z. L. Cheng, R. Skouta, R. A. Friesner, L. Venkataraman, R. Breslow, *J. Am. Chem. Soc.* **2011**, *133*, 2136–2139.
- [34] L. Venkataraman, Y. S. Park, A. C. Whalley, C. Nuckolls, M. S. Hybertsen, M. L. Steigerwald, *Nano Lett.* **2007**, *7*, 502–506.
- [35] S. Y. Quek, M. Kamenetska, M. L. Steigerwald, H. J. Choi, S. G. Louie, M. S. Hybertsen, J. B. Neaton, L. Venkataraman, *Nat. Nanotechnol.* **2009**, *4*, 230–234.
- [36] X. Y. Xiao, B. Q. Xu, N. J. Tao, *Nano Lett.* **2004**, *4*, 267–271.